

## SUMMARY OF THE U15 PROTOTYPE MAGNETIC PERFORMANCE

M. Calvi, M. Aiba, M. Brügger, S. Danner, R. Ganter, C. Ozkan, Th. Schmidt,  
PSI, Villigen, Switzerland

### *Abstract*

The first undulator prototype for SwissFEL (U15) was assembled and magnetically tested. The measurement instrumentations and the algorithms developed for the undulator optimization are presented and a comparison among different approaches is reviewed. The magnetic measurement results before and after the installation of the vacuum components are discussed. The summary of the undulator test with 100 MeV electron beam is presented and the impact of the radiation on the magnetics is addressed.

### INTRODUCTION

The U15 design has been developed specifically for the SwissFEL project. Both the hard and the soft X-ray lines will be equipped with undulators built with the same frame and gap drive system.

To optimize the undulator stiffness and its dimensions a close frame has been implemented. This feature makes the undulator more compact but it required the development of a new magnetic measurement bench to optimize the structure.

Two new benches were developed based on SAFALI system [1]: the first is used without the vacuum chamber during the optimization phase and the second one with the vacuum chamber for phase adjustment and final checks before the installation in the tunnel.

The large number of undulator modules required per beamline (12 for Aramis I) increases substantially the effort associated with the magnetic shimming compared to a synchrotron where a beamline consists usually of a single module. To mitigate this issue and the cost associated, the support of the magnetics has been designed more flexible. It is now possible to precisely adjust the pole heights in the range of micrometers by means of a flexor driven by a wedge-screw system.

Before the series production a prototype was built to validate the new design approach. It was extensively tested and magnetically optimized before the installation into the SwissFEL Injector Test Facility of PSI. This last activity aimed to a better integration of the undulator hardware within the rest of the accelerator components as well as to test the field quality directly with the electron beam. The impact of the radiation on both the magnetics and electronics was monitored. In the following all these activities are discussed in view of the series production.

### MAGNETIC MEASUREMENT INSTRUMENTATION

There are two main systems used for the magnetic measurements of the undulators, the Hall sensors and the moving wire. The first is used to estimate the field profile

and to calculate the trajectory and the phase error; the second is needed to measure the field integrals and the earth field in the laboratory (this measurement is performed before installing the undulator). The first field integral and the earth field are also used to calibrate the data measured with the Hall sensors. A zero Gauss chamber is planned for a systematic cross check during the production phase. A third system, the so-called pulsed wire, is also available but it is not planned to be used on a regular basis and it is not discussed in the following.

### *Hall Sensor Measurement Benches*

A Hall probe is used to measure the magnetic field profile along or parallel to the undulator axis. The probe is built of three Hall sensors to measure the three components of the field. They are embedded in a ceramic support and aligned to the direction of the measurement axis and spaced of 2 mm.

To precisely follow the undulator axis the probe is guided with lasers. The two beams pass through two pinholes attached to the probe. The transmitted light carries the information about its position. This information is detected by two position sensitive diodes (PSD) and used to correct the trajectory of the probe. This logic is implemented in a feedback loop and optimized to decrease the measurement noise produced by the vibrations.

As already previously mentioned there are two different Hall sensor benches with two specific applications.

The one used for the optimization (bench A) is not constrained by the vacuum chamber and its implementation is more comfortable. A linear motor is used to displace the probe and the electronics. This last feature has the advantage to reduce the cable length and to have a fix connection between the probe and the ADC.

The measurements after the installation of the vacuum chamber (bench B) require more integration efforts. A piezoelectric-motor has been implemented in place of the linear motor because of the reduced dimensions. These actuators are usually made for travel shorter than a meter and the ceramic supports where the two piezoelectric legs actually “walk” are produced only for short length. Custom manufacture is possible but expensive and fragile. The solution implemented consists of several ceramic supports glued along the measuring bench and a piezoelectric motor with four legs to easily overcome the junction region between ceramic modules.

### *Moving Wire Bench*

The moving wire bench has been modified and improved with respect to the system available at the SLS. A set of servomotors has been implemented in place of the steppers used previously to move the stages. This

choice allowed higher speed and smoother motion (i.e. more uniform velocity). A Keithley nano-volt meter is now used to read out the induced voltage while the wire is moving. The integral (Bdl) is then simply equal to the voltage divided by the speed in each instantaneous wire position.

## OPTIMIZATION ALGORITHMS

The optimization of the magnetic structure can start when all the data available from the measurement campaign are ready and analysed. There are no direct specifications on the field profile and it is easier and more convenient to operate directly on the trajectory and phase errors. The shimming is based on the individual pole height adjustment applied by means of a robot. A second and coarser knob is the adjustment of the columns height to locally tune the field strength, i.e. the phase error.

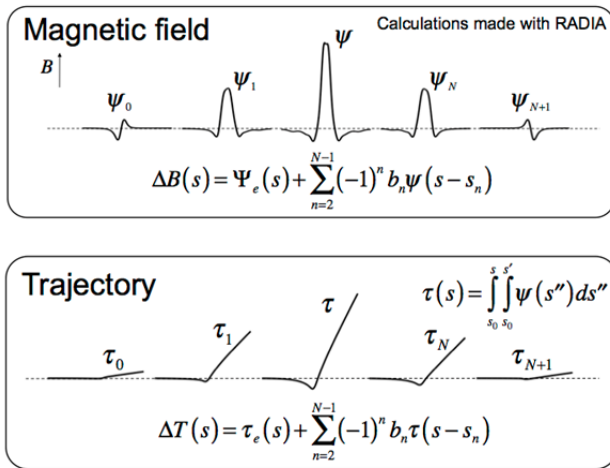


Figure 1: On the upper picture the calculated field variation (RADIA code) due to pole height variations and on the bottom the correspondent trajectory corrections. On the centre of both pictures it is represented the changes in the periodic part of the array, on the sides the impact of the poles in the extremities (the last two screws in both sides).

### Trajectory Optimization

Integrating twice the magnetic field profile along the longitudinal coordinate gives, after an appropriate normalization, the trajectory. The straightness of the trajectory is one of the main requirements for a FEL to guarantee the overlap between electrons and photons. For the SwissFEL, a maximum trajectory deviation of 2 μm RMS is specified.

The straightness is an intuitive requirement and it can be also quantified. The electron wiggling around a straight line represents the ideal trajectory and any deviation is accounted as an error. One of the ways to estimate the deviation is to convolute the calculated trajectory with a window function with a width equal to the undulator period length. This approach is very effective for the majority of the trajectory but it fails in giving an accurate estimation in the end regions where

there is no periodicity. For the first and last period the optimization was done following a more pragmatic approach, calibrating this knob experimentally and finding the right correction with an iterative procedure.

An algorithm estimates the local pole height corrections. It requires first the knowledge of the field change caused by the local corrections. These are calculated with the computer code RADIA, see Fig. 1. In the limit of small corrections (field change < 1%) the hypothesis of linear superposition is accurate and it simplifies the optimization process. Knowing the trajectory deviation, it is then possible to calculate the full set of adjustments.

### Phase Optimization

A perfect trajectory is not enough to fulfill the requirement of a FEL and the phase error, which measures the accuracy of the electron-photon resonance condition, should also be taken into account. The phase error calculation is quite standard and it can be found in any textbook on the subject [2]. To reduce ambiguity it is relevant to highlight that the deviation from the ideal synchronization is estimated only for the photons which correspond to the zeros of the first field integral. As discussed previously for the trajectory, it is also possible to estimate the impact of each pole height change on the phase and sum them up with some approximations. In Fig. 2 the local phase correction is calculated for a pole height change. When the local field is increased the phase undergoes a local step function plus an oscillating tail.

The height of the columns can also be changed to correct the phase error. It is a coarser correction than the pole height correction because it is localized over a region of about half a meter. The optimization algorithm previously described is also used to estimate the column adjustment, based on the ANSYS calculation of the deformation induced.

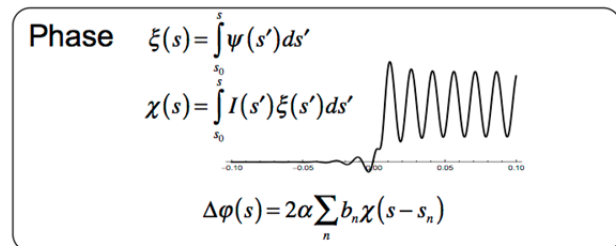


Figure 2: The phase change due to pole height variation, this calculation is relevant only for the periodic part of the undulator field.

## MAGNETIC MEASUREMENT RESULTS

The U15 prototype was an important test for the new set of magnetic measurement benches and optimization procedure in view of the series production.

The assembly of the magnetic array into the frame is completed at PSI before moving the undulator to the bench A. There the undulator is aligned mechanically to the bench by mean of 5-axis movers. The height and the

pitch are further aligned based on magnetic field measurements. Then the undulator is optimized at the nominal gap ( $K=1.2$ ) and then the magnetic field is measured for all gaps. The trajectories and the phase errors are calculated to check how they scale with gap and if further correction actions are required. Then the undulator is moved out of the bench and the magnetic array disassembled from the frame. The vacuum components are installed around the array and moved back to the frame. The completed undulator assembly is then moved to the measuring bench B for the phase error optimization and final characterization. This last action requires the same environmental conditions experienced in the tunnel to produce reliable data to be used later in the machine operation.

In the following the results of the first complete measurement campaign are reported with some additional information concerning the qualification of the measuring systems.

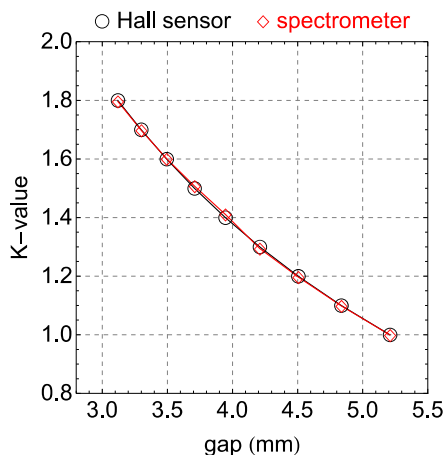


Figure 3: The K-value is measured as a function of the gap with two independent systems: in black the values estimated with the magnetic measurements (Hall sensors) and in red the value measured with the spectrometer during the test in the SwissFEL injector accelerator.

### K-value versus Gap Measurements

The first parameter to be verified is the K-value; in Fig. 3 the K-value versus gap is reported. The curve is fitted with the standard function used for hybrid structure. The reproducibility of the measurement is better than 0.01% while the absolute accuracy of the probe is 0.25%.

### Trajectory Measurements

In the optimization procedure selected for the prototype, the trajectory is the first parameter that shall be optimized. In Fig. 4 an example of the results obtained after a single correction is presented where no further iterations are required. This is feasible because of the accuracy of the magnetic model and the precision of the applied corrections, only conceivable with the help of an angular encoder. This successful result is valid only for the nominal gap while in Fig. 5 the trajectory for all operational relevant gaps ( $K>1$ ) is reported. The

corrections applied do not scale ideally for all gaps but the results are well within the specifications.

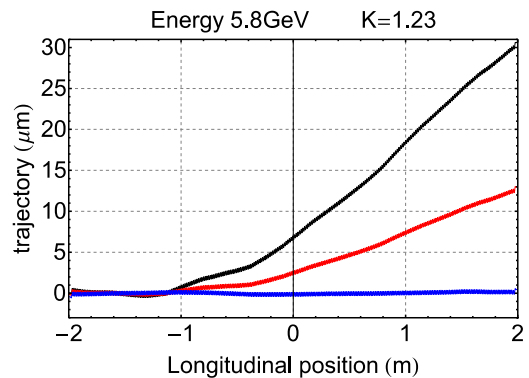


Figure 4: The trajectory measurements before (black), during (red) and after the optimization (blue) for nominal gap.

The trajectories after the assembling of the vacuum components show some changes. For instance the first field integral is  $200 \text{ G}\times\text{cm}$  different and this requires further investigations. The preliminary conclusion is that the assembly work had a negligible impact and the main perturbation comes from the magnetic field produced in the magnets present in the vacuum pumps. It was demonstrated that it is possible to minimize this impact with an appropriate swapping of those magnets. This is a time consuming procedure and it should be as much as possible avoided. The layout of the vacuum chamber has been redesigned and now it allows moving the pumps further out from the beam axis if necessary.

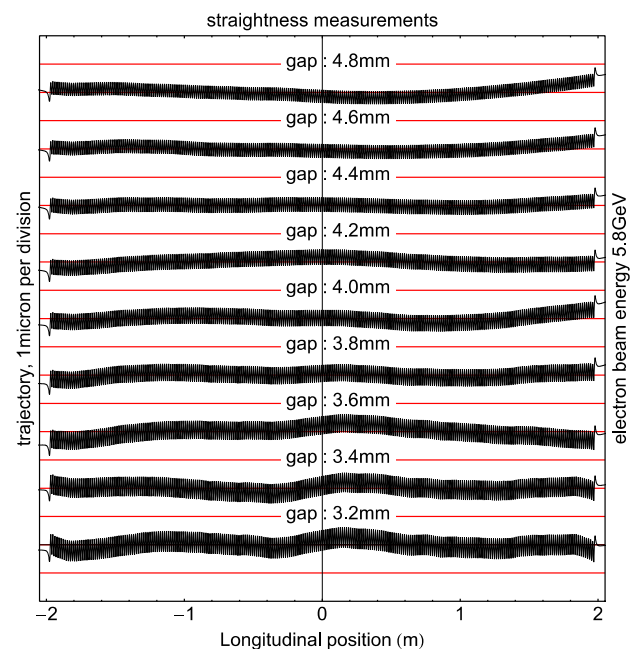


Figure 5: The trajectory straightness for different gaps. Residual entrance and exit kicks are not represented in this picture.

### Phase Error Measurements

The phase was optimized after the correction of the trajectory, starting with the coarse knob represented by the column height adjustment. This was enough to minimize the RMS phase error well below the requirements. To investigate the limit of the approach the phase was further improved using pole height adjustment. At the end of this campaign the RMS phase error was about 2.3 at nominal gap. This was an excellent result and very encouraging towards the series production. Unfortunately the corrections did not last while changing the gap. After a “field cycle” (nominal gap, fully open gap, fully close gap, nominal gap) the phase was changing up to unacceptable values (measured up to 14°). This problem is now identified and well understood: it is originated in the locking mechanism. The height of the columns is adjusted by mean of a differential screw and then locked with a counter nut. In the original design only one counter nut was foreseen which is not enough to block the play in both sides of the screw. A second nut was then designed and a fully column assembly tested. The two sides of the device are now behaving as a single solid object. The final test of the undulator with the new columns is planned for the end of 2014.

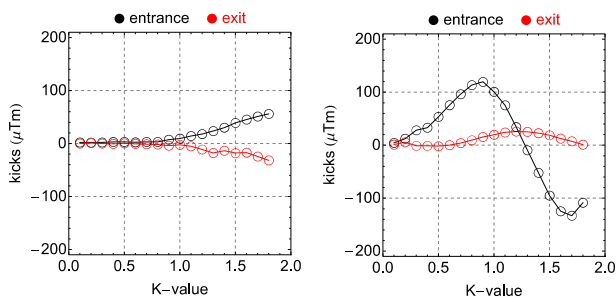


Figure 6: On the left side equivalent the entrance and exit kicks on the horizontal plane and on the right on the vertical plane.

### TEST IN THE INJECTOR

The U15 prototype was tested also with a low energy electron beam (maximum 250 MeV) at the PSI injector test facility. The layout of the accelerator was adapted to this test, one 5 m long girder was removed to gain space for the undulator and the adjacent girders reshuffled to allocate the instrumentation. In the following only the tests and results relevant to evaluate the magnetic performance are presented.

Two upstream BPMs and two downstream BPMs are installed to monitor the position and angle of the beam before and after the undulator. A spectrometer for visible light is installed downstream the undulator to measure the photon energy (this test was performed at a reduced electron energy of 100 MeV).

The first action is the definition of a reference orbit, followed by the beam-based alignment of the undulator by mean of two dedicated quadrupoles. These last are pre-aligned during the magnetic measurement and keep track

of the undulator axis: one is just at the entrance of the undulator and one at the exit.

### BPMs

The first and second field integrals of the undulator can be estimated from the orbit measurements. The BPMs are sorted for this convenience and to simplify the task all quadrupole in between the BPMs are switched off and only corrector up-stream the undulator are used to keep a constant injection orbit. The analysis of the data is summarized in Fig. 6, where the first and second field integrals are represented as an equivalent entrance and exit kick (assuming no kick for fully open gap).

The results for the horizontal plane show the signature of the central symmetry of the field profile, which is not shadowed by the field error. The kick magnitude is comparable to the calculated values and the results of the magnetic measurements.

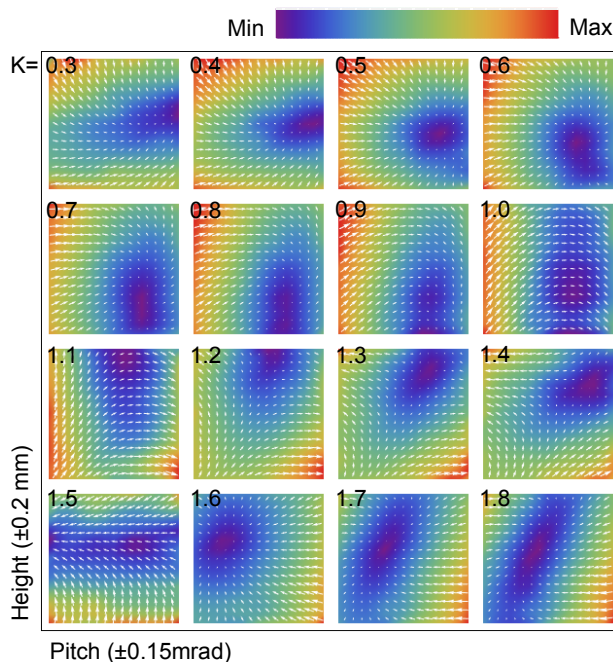


Figure 7: The center (deep purple colored) of the vertical quadrupole component for different K-values, starting from the top left with  $K=0.3$ , down to the right bottom with  $K=1.8$ . The individual plots represent the first and second field integral (the x and y components of the white arrows respectively) as a function of the undulator pitch and height.

On the vertical plane this preliminary analysis shows kicks larger than expected. The functional relation between the field errors and the K-values carries the signature of the quadrupole component. The undulator vertical focusing cannot be neglected at the operating energy of the injector and extra set of data is produced to better characterize this feature and as far as possible to disentangle the two effects. The estimation of the vertical kicks is repeated for different undulator height and several K-values, see Fig. 7. In this plane (pitch-

height) the quadrupole component displays very clearly and the phase advance changes for different K-value.

The axis of the quadrupole component moves for different K-values and this can be explained only by field errors. The dynamic described by the center indicates also that the field errors change with the gap.

### *Spectrometer*

Operating the injector at 100 MeV produces photons in the visible and it gives the opportunity to use a simple spectrometer in air to characterize the radiation energy/wavelength. As presented in Fig. 3 this measurement provides the opportunity to cross check the estimation of K-values versus gap previously estimated with the hall sensors in the laboratory. The good agreement confirms the magnetic design and the quality of the new magnetic measurement bench.

### *Radiation Measurements*

The radiation level was constantly monitored during the entire test. This information was available in the control

room and used to minimize the dose on the hardware. After the 3 months period the integrated dose absorbed was estimated to be about 100 Gray and there was no impact observed neither in the magnetics nor in the electronics.

## CONCLUSION

The test of the U15 prototype was an important milestone for the SwissFEL project. The original design was assessed, some residual problems were discovered and working solution implemented.

## REFERENCES

- [1] T. Tanaka et al., "In-situ Undulator Field Measurement with the SAFALI System", in Proc. 29<sup>th</sup> Int. Free-Electron Laser Conf. , Novosibirsk, 2008, p. 467-471.
- [2] J. A. Clarke, "The Science and Technology of Undulators and Wigglers", Oxford Science Publications, 2004.